Molecular Physics
Vol. 00, No. 00, Month 2009, 1–11

Special Issue in honour of Luciano Reatto

Two component bosonic Josephson junctions in elongated traps

M. Melé-Messeguer[a*], B. Juliá-Díaz[a,b] , M. Guilleumas[a] and A. Polls[a]

[a]Dept. d'Estructura i Constituents de la Matèria, U. Barcelona, 08028 Barcelona, Spain;

[b]ICFO The Institute of Photonic Sciences, 08860 Castelldefels, Spain

(*June 2011*)

We study binary mixtures of Bose-Einstein condensates confined in a two-well potential within the framework of the Gross-Pitaevskii equation. We reexamine both the single component and the binary mixture cases for such a potential. We investigate the most usual dimensional reductions used to solve the Gross-Pitaevskii equations, including the one proposed by Reatto and collaborators. To this end, we compare numerical simulations of the 1D reductions with the full 3D numerical solutions of the Gross-Pitaevskii equation. Our analysis considers an experimentally feasible binary mixture of an $F = 1$ spinor condensate where two of its Zeeman manifolds are populated.

Keywords: BECs, Josephson junctions, Condensates, double-well potentials

1. Introduction

The first evidence of phase coherence of a BEC was obtained in early experiments [1] where clean interference patterns appeared in the overlapping region of two expanding condensates. It has been only recently that clear evidence of an external bosonic Josephson junction in a weakly linked scalar (single component) BEC has been experimentally reported, first by the group of M. Oberthaler in Heidelberg [2], followed by the group of J. Steinhauer [3]. Internal Josephson dynamics has also been experimentally achieved [4].

In the experiment of Ref. [2], two condensates are confined in a double-well potential with an initial population imbalance between both sides which triggers the Josephson oscillations. The tunneling of particles leads to a coupled dynamical evolution of the two conjugate variables, the phase difference between the two weakly linked condensates and their population imbalance. In spite of the system being dilute, the atom-atom interaction plays a crucial role in the Josephson dynamics, leading to new regimes beyond the standard Josephson effect, e.g. macroscopic quantum self-trapping (MQST).

The Gross-Pitaevskii (GP) theory provides an appropriate framework for investigating Josephson dynamics in weakly interacting systems provided: (a) the number of atoms is large enough so that quantum fluctuations can be neglected, and (b) the initial many-body state is of mean-field type. Josephson oscillations in scalar Bose-Einstein condensates were initially studied by [5, 6], and since then they have been studied using different techniques, for a review see [7]. For $N \lesssim 100$, the

*Corresponding author Email: marina@ecm.ub.es

ISSN: 0026?8976 print/ISSN 1362?3028 online

DOI: 10.1080/0026897YYxxxxxxxx
http://www.informaworld.com

exact Josephson dynamics has been recently shown to depart from the mean-field Gross-Pitaevskii, as seen in the evolution of the population imbalance or with the appearance of fragmentation [8]. For small N the transition from Josephson to self-trapped dynamics has also been shown to involve the appearance of strongly correlated quantum states [9]. For larger number of atoms, $N \gtrsim 1000$ the full three dimensional time-dependent Gross-Pitaevskii equation (**GP3D**) provides a reasonable agreement with the experimental data of Ref. [2], see Refs. [7, 10], where $N \sim 1150$ and the system is let to evolve for less than a Rabi time.

However, since 3D dynamics need in general rather involved calculations, one can benefit from the fact that the barrier is created along one direction and the tunneling of particles is mainly one dimensional (1D) to investigate the Josephson dynamics by means of effective 1D GP-like equations. Among these reduced GP equations, the non-polynomial nonlinear Schrödinger equation (**NPSE**) proposed by Prof. Reatto and collaborators in Ref. [11] has provided the best agreement with the experimental results in scalar condensates, whereas another effective 1D Gross-Pitaevskii equation (**GP1D**) fails to describe the dynamics for large number of trapped atoms in the same trapping conditions as in the Heidelberg's experiment [7].

Josephson oscillations in binary mixtures confined in double-well potentials have been addressed in a number of recent articles. The case of two-component BECs with density-density interactions has been studied within two-mode approaches in Refs. [12–19]. Ref. [17] goes one step further and also considers **GP1D** simulations. Spin-dependent interactions have been addressed in Refs. [20–22]. In Refs. [20, 23] the interest of studying Josephson dynamics in binary mixtures has been emphasized as it can give access to information of the different scattering lengths present in the system.

The paper is organized as follows. The coupled Gross-Pitaevskii equations for a binary mixture are presented in Sect. 2 , as well as the different one-dimensional reductions of the **GP3D** equations for the mixture: **GP1D** and **NPSE** . In Sect. 3 we review results for the single component case. And in Sect. 4, we discuss the dynamics of a bosonic binary mixture in a double-well potential with the same parameters as in the experiment [2]. Finally, the conclusions are presented in Sec. 5.

2. Mean field approach: Gross-Pitaevskii equations

We consider a binary mixture of weakly interacting bosons at zero temperature, confined by a symmetric double-well potential, $V(\mathbf{r})$. For dilute systems with large enough number of particles, the Gross-Pitaevskii equation provides a suitable framework to study the dynamics. In the mean field approximation, each condensate is described by the corresponding wave function $\Psi_i(\mathbf{r};t)$, with $i = a, b$ denoting each of the two components of the binary mixture. In most situations, the system will behave as if there were four weakly linked Bose-Einstein condensates, two per each component of the binary mixture per each side of the potential barrier. The mean field description will reflect this feature by the homogeneous quantum phase of $\Psi_i(\mathbf{r};t)$ at each side of the potential barrier.

The dynamical evolution of the two wave functions can be obtained by solving the two coupled GP equations:

$$i\hbar\frac{\partial\Psi_a(\mathbf{r};t)}{\partial t}=\left[-\frac{\hbar^2}{2m_a}\nabla^2+V(\mathbf{r})+g_{aa}N_a|\Psi_a(\mathbf{r};t)|^2+g_{ab}N_b|\Psi_b(\mathbf{r};t)|^2\right]\Psi_a(\mathbf{r};t)$$
$$i\hbar\frac{\partial\Psi_b(\mathbf{r};t)}{\partial t}=\left[-\frac{\hbar^2}{2m_b}\nabla^2+V(\mathbf{r})+g_{ba}N_a|\Psi_a(\mathbf{r};t)|^2+g_{bb}N_b|\Psi_b(\mathbf{r};t)|^2\right]\Psi_b(\mathbf{r};t). \quad (1)$$

For each component, the condensate wave function $\Psi_i(\mathbf{r};t)$ is normalized to 1, m_i is the atomic mass, and $g_{ii}=4\pi\hbar^2a_i/m_i$ is the effective atomic interaction between atoms of the same species, with a_i the corresponding s-wave scattering length. The coupling between both components is governed by the inter-species interaction $g_{ab}\equiv g_{ba}$, which depends on the specific nature of the binary mixture. The total number of atoms in the mixture is $N=N_a+N_b$.

We will consider binary mixtures made of $F=1$ ^{87}Rb atoms populating the $m=\pm1$ Zeeman sublevels. This implementation simplifies the dynamics as the inter- and intra-species couplings are similar in magnitude. Of course this choice limits the phenomena which can be observed. On the other hand its simplicity allows to discuss the different dimensional reductions of the 3D equations taken in the literature.

We consider the same setup and the same trap parameters as in the experiments of the Heidelberg group [2]. There, a condensate of ^{87}Rb with 1150 atoms is confined to a fairly small region of $\sim 5\,\mu$m through the potential,

$$V(\mathbf{r})=\frac{1}{2}M(\omega_x^2x^2+\omega_y^2y^2+\omega_z^2z^2)+V_0\cos^2(\pi x/q_0) \quad (2)$$

with $\omega_x=2\pi\times 78$ Hz, $\omega_y=2\pi\times 66$ Hz, $\omega_z=2\pi\times 90$ Hz, $q_0=5.2\mu$m, and $V_0=413\,h$ Hz.

In the full **GP3D** simulations we define the number of atoms in the left well as: $N_L(t)=\int_{-\infty}^{0}dx\int_{-\infty}^{\infty}dy\int_{-\infty}^{\infty}dz\;|\Psi(\mathbf{r};t)|^2$. The number of atoms in the right well is computed as $N_R(t)=N-N_L(t)$. From these values, the population imbalance reads, $z(t)=(N_L(t)-N_R(t))/N$. Analogous definitions are used in the **GP1D** and **NPSE** equations.

The phase at each side side of the potential barrier is obtained in the following way. The phase at each point at a certain time, $\phi(x,y,z;t)$, is: $\Psi(x,y,z;t)=\sqrt{\rho(x,y,z;t)}\exp(\imath\;\phi(x,y,z;t))$, where the local density is $\rho(x,y,z;t)=|\Psi(x,y,z;t)|^2$. Averaged densities, integrating over the z component, are defined as $\rho(x,y;t)=\int_{-\infty}^{\infty}dz\;\rho(x,y,z;t)$.

To visualize the phase coherence along some of the planes we define an average phase, integrating the z component, as $\phi(x,y;t)=\frac{1}{\rho(x,y;t)}\int_{-\infty}^{\infty}dz\;\rho(x,y,z;t)\;\phi(x,y,z;t)$. The phase on the left, $\phi_L(t)$, is defined as,

$$\phi_L(t)=\frac{1}{N_L(t)}\int_{-\infty}^{0}dx\int_{-\infty}^{\infty}dy\int_{-\infty}^{\infty}dz\;\rho(x,y,z;t)\;\phi(x,y,z;t). \quad (3)$$

The phase on the right, $\phi_R(t)$, is defined accordingly. The phase difference between each side of the barrier is computed as $\delta\phi(t)=\phi_R(t)-\phi_L(t)$.

2.1. *One dimensional Gross-Pitaevskii-like equations (***GP1D** *)*

Assuming that most of the dynamics takes place in the direction which contains the barrier, the x direction in our case, one can approximate the wave function

of the system by $\Psi(x,y,z;t) \sim \Psi^{1D}(x;t)\ \varphi_{g.s.}(y)\ \varphi_{g.s.}(z)$, where $\varphi_{g.s.}$ are the corresponding ground state wave functions for the trapping potential in the y or z direction in absence of interactions. In this way it can be shown [24] that in the case of one component system, $\Psi^{1D}(x;t)$ fulfills a Gross-Pitaevskii-like 1D equation,

$$i\hbar\frac{\partial\Psi^{1D}(x;t)}{\partial t} = \left[-\frac{\hbar^2}{2m}\partial_x^2 + V(x) + g_{1D}N|\Psi^{1D}(x;t)|^2\right]\Psi^{1D}(x;t)\,, \tag{4}$$

where the corresponding 1D coupling constant is obtained rescaling the 3D one, $g_{1D} = g/(2\pi a_\perp^2)$, being $a_\perp$ the transverse oscillator length, $a_\perp = \sqrt{\hbar/m\omega_\perp}$, with $\omega_\perp = \sqrt{\omega_z\omega_y}$.

The extension to binary mixtures (and also to spinor condensates [25]) may be written down readily,

$$\begin{aligned} i\hbar\frac{\partial\Psi_a^{1D}(x;t)}{\partial t} &= \left[-\frac{\hbar^2}{2m}\partial_x^2 + V(x) + \sum_{j=a,b} g_{a\,j;1D}N_j|\Psi_j^{1D}(x;t)|^2\right]\Psi_a^{1D}(x;t) \\ i\hbar\frac{\partial\Psi_b^{1D}(x;t)}{\partial t} &= \left[-\frac{\hbar^2}{2m}\partial_x^2 + V(x) + \sum_{j=a,b} g_{b\,j;1D}N_j|\Psi_j^{1D}(x;t)|^2\right]\Psi_b^{1D}(x;t) \end{aligned} \tag{5}$$

where, the rescaled couplings are $g_{ij;1D} = g_{ij}/(2\pi a_\perp^2)$.

2.2. *Non-polynomial Schrödinger equation (***NPSE***)*

A more sophisticated reduction that includes to some extent the transverse motion of the elongated BEC in the corresponding potential is the so-called non-polynomial Schrödinger equation, proposed for a scalar BEC by Prof. Reatto and collaborators [11]. The **NPSE** recovers the previously discussed 1D reduction in the weakly interacting limit, but it has been shown to provide the best agreement with the experimental results on Josephson oscillations between two coupled BECs [22]. The **NPSE** for the one-component case reads,

$$\begin{aligned} i\hbar\frac{\partial\Psi(x;t)}{\partial t} = \Bigg[&-\frac{\hbar^2}{2m}\partial_x^2 + V(x) + g_{1D}\frac{N|\Psi(x;t)|^2}{\sqrt{1+2a_sN|\Psi(x;t)|^2}} \\ &+ \frac{\hbar\omega_\perp}{2}\left(\frac{1}{\sqrt{1+2a_sN|\Psi(x;t)|^2}} + \sqrt{1+2a_sN|\Psi(x;t)|^2}\right)\Bigg]\Psi(x;t)\,, \end{aligned} \tag{6}$$

The generalization of the **NPSE** for two components in a binary mixture of BECs has been addressed in Ref. [26]. The system of equations, which become rather involved, can be further simplified in the case of equal interactions, both intra- and inter-species:

$$\begin{aligned} i\hbar\frac{\partial\Psi_j(x;t)}{\partial t} = \Bigg[&-\frac{\hbar^2}{2m_j}\partial_x^2 + V + g_{1D}\frac{\rho(x;t)}{\sqrt{1+2a_s\rho(x;t)}} \\ &+ \frac{\hbar\omega_\perp}{2}\left(\frac{1}{\sqrt{1+2a_s\rho(x;t)}} + \sqrt{1+2a_s\rho(x;t)}\right)\Bigg]\Psi_j(x;t) \end{aligned} \tag{7}$$

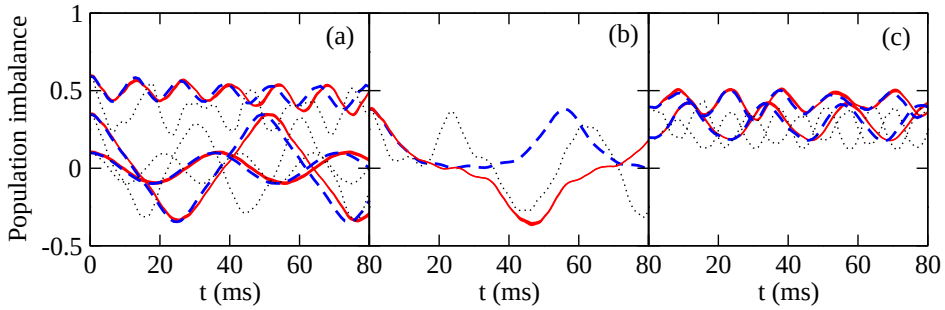

Figure 1. Dynamical evolution of the population imbalance, z, between both sides of the barrier for a single component condensate. Solid (red) line corresponds to the **GP3D**, the dashed (blue) line to the **NPSE**, and the dotted (black) stands for the **GP1D**. Panel (a) contains $\delta\phi(0) = 0$ cases, with $z(0) = 0.1, 0.35$, and 0.6. (b) Corresponds to the critical value, $z(0) = 0.39$ and $\delta\phi(0) = 0$. (c) Depicts two self-trapped cases with an initial $\delta\phi(0) = \pi$, with $z(0) = 0.2$, and 0.4.

where $\rho(x;t) = N_a|\Psi_a(x;t)|^2 + N_b|\Psi_b(x;t)|^2$, $j = a, b$, and, as before, $g_{1D} = g/(2\pi a_\perp^2)$, $g \equiv g_{aa} = g_{bb} = g_{ab} = g_{ba}$, and $\int dx|\Psi_j(x)|^2 = 1$.

3. Numerical results for a single component condensate

First, let us consider the case of a single component condensate. In Fig. 1 we present the time evolution of the population imbalance for Josephson, and self-trapped regimes. We compare the full **GP3D** (solid red) with the two 1D reductions, **GP1D** (dotted black) and **NPSE** (dashed blue).

The first panel, (a), contains simulations performed with zero initial phase difference, i.e. Josephson oscillations and self-trapping cases. For the Josephson cases, $z(0) = 0.1, 0.35$, the imbalance oscillates with a frequency which is mostly independent of the initial imbalance (for small imbalances). With $z(0) = 0.1$ the oscillations are almost sinusoidal, while as we increase the initial imbalance their shape becomes more involved but remaining periodic. In the self-trapped case, $z(0) = 0.6$, the atoms remain mostly on their initial side of the trap and there are short and small periodic oscillations as predicted by two-mode models [5]. At longer times, the imbalance is seen to decrease smoothly, implying a departure from the predicted two-mode dynamics.

The two 1D reductions give in most situations qualitatively similar results as the **GP3D**, but not quantitatively in all cases. The **NPSE** is seen to reproduce very well the **GP3D** in all the runs up to times near $\sim$ 40 ms. Above those times, the period of oscillation predicted by the **NPSE** is slightly shorter than the **GP3D** one. The **GP1D** on the contrary only captures the amplitude of oscillation in the Josephson dynamics, failing in all cases to give the same period as the **GP3D** or the **NPSE**. Moreover, the **GP1D** departs notably from the **GP3D** for the self-trapped case.

Panel (b) is computed very close to the critical value for the appearance of self-trapping in the full **GP3D**, $z(0) = 0.39$ for $\delta\phi(0) = 0$. The **GP1D** and **NPSE** predict a critical initial imbalance close to the **GP3D** value.

Panel (c) contains two self-trapped cases obtained with an initial $\delta\phi(0) = \pi$ and $z(0) = 0.2$, and 0.4. Notice that for $\delta\phi(0) = \pi$ the critical imbalance is smaller than for $\delta\phi(0) = 0$. The discussion is similar to the Josephson case, i.e. the **NPSE** captures most of the dynamical features of the **GP3D** while the **GP1D** only provides a qualitative understanding of the problem.

To further explore the quality of the 1D reductions, we present in Fig. 2 the density profiles in the x direction after integrating the y and z components, $\rho(x;t) = \int_{-\infty}^{\infty} dy \int_{-\infty}^{\infty} dz\, |\Psi(x,y,z;t)|^2$ at $t = 50$ ms. The agreement between the **NPSE** and

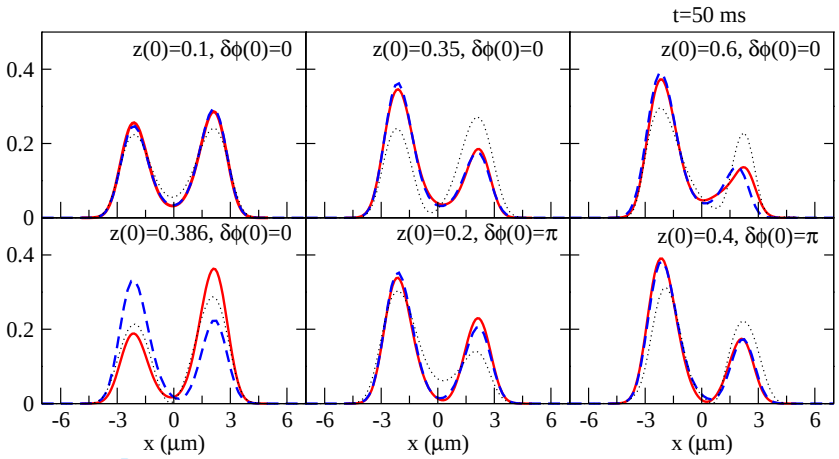

Figure 2. Snapshots of the axial density profiles, $\rho(x;t)$ $(\mu m)^{-1}$ at $t = 50$ ms calculated by means of the **GP3D** evolution (solid red line), the **NPSE** (dashed blue line), and the **GP1D** (dotted black line). The initial conditions correspond to the ones used to generate Fig. 1.

the **GP3D** is very good in most situations, except for the critical case, as expected. In all cases the density profiles show a clear bi-modal structure. The **GP1D** does not predict the correct density profiles and, as seen in the self-trapped case, $(z(0) = 0.6, \delta\phi(0) = 0)$, does show the contribution of higher modes. The critical initial imbalance starting with no phase difference that we find numerically by means of the **GP3D** is the same as found in Ref. [10], $z_c = 0.39$, and differs from the one reported in Ref. [2], $z_c = 0.5$. The agreement of the **NPSE** with **GP3D** results justifies the use of **NPSE** in Ref. [2] to analyze their experiment.

4. Numerical solutions of the 3D Gross-Pitaevskii equations: binary mixture

As discussed in Sec. 2, one feasible way of experimentally prepare binary mixtures of BECs is to consider a number of atoms populating the $m = \pm 1$ Zeeman components of an ^{87}Rb $F = 1$ spinor. The experimental observation of Josephson tunneling phenomena by the Heidelberg group seems to be possibly extended to trap both Zeeman components. In this case the two components of the mixture have the same mass, $M \equiv m_a = m_b$, and equal intra-species interactions, $g_{aa} = g_{bb} \equiv g$. With respect to the inter-species interaction we will consider the case of ^{87}Rb which implies $g_{ab} \sim g$.

The mean field **GP3D** system of equations governing the dynamics of the three components of an $F = 1$ spinor BEC can be written as [27],

$$
\begin{aligned}
i\hbar\frac{\partial\psi_{\pm1}}{\partial t} &= [\mathcal{H}_s + c_2(n_{\pm1} + n_0 - n_{\mp1})]\psi_{\pm1} + c_2\psi_0^2\psi_{\mp1}^*\,, \\
i\hbar\frac{\partial\psi_0}{\partial t} &= [\mathcal{H}_s + c_2(n_1 + n_{-1})]\psi_0 + c_2 2\psi_1\psi_0^*\psi_{-1}\,,
\end{aligned}
\tag{8}
$$

with $\mathcal{H}_s = -\hbar^2/(2M)\,\boldsymbol{\nabla}^2 + V + c_0 n$ being the spin-independent part of the Hamiltonian. The density of the m-th component is given by $n_m(\mathbf{r}) = |\psi_m(\mathbf{r})|^2$, while $n(\mathbf{r}) = \sum_m |\psi_m(\mathbf{r})|^2$ is the total density normalized to the total number of atoms N. The couplings are $c_0 = 4\pi\hbar^2(a_0 + 2a_2)/(3M)$ and $c_2 = 4\pi\hbar^2(a_2 - a_0)/(3M)$, where a_0 and a_2 are the scattering lengths describing binary elastic collisions in the channels of total spin 0 and 2, respectively. Their values for ^{87}Rb are $a_0 = 101.8a_B$ and $a_2 = 100.4a_B$ [28]. Since the spin-dependent coupling, c_2, is much smaller than the spin-independent one, c_0, and the total number of atoms that we will consider

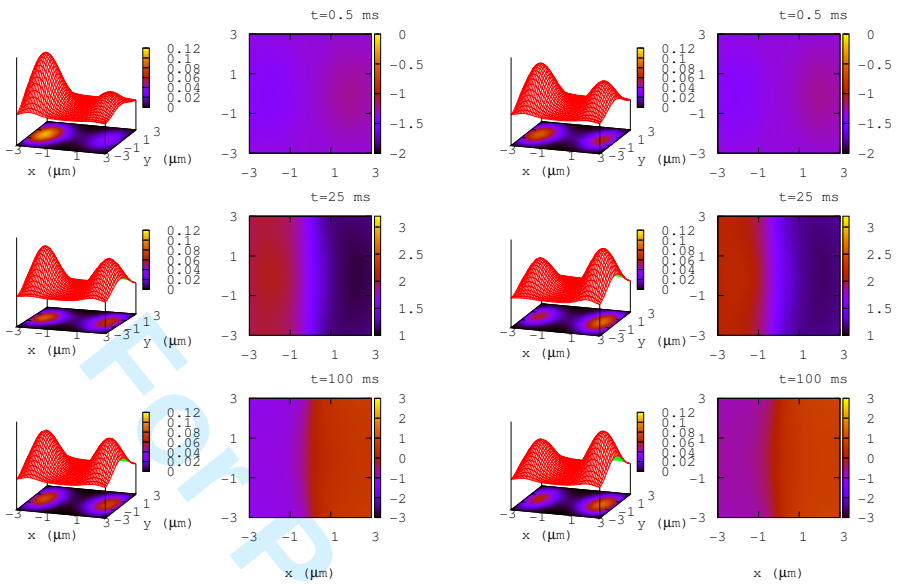

Figure 3. Full **GP3D** calculations of the dynamics of a binary mixture with $z_a(0) = 0.5$, $z_b(0) = 0.2$, $\delta\phi_a(0) = 0$, $\delta\phi_b(0) = 0$, $f_a = 0.25$ and $f_b = 0.75$. Each row contains from left to right: 3D depictions complemented by contour plots of $\rho_a(x, y; t)$, a contour plot of the averaged phase $\phi_a(x, y; t)$, 3D depictions complemented by contour plots of $\rho_b(x, y; t)$, and a contour plot of the averaged phase $\phi_b(x, y; t)$. Each row corresponds to a different time, 0.5 ms (upper), 20 ms (middle) and 60 ms (lower), respectively.

is relatively small $N = 1150$, the population transfer between the different components can be neglected [20]. Therefore, in our calculation the number of atoms in each sublevel remains constant in time allowing to treat the system as a binary mixture of components a and b. Comparing the system of Eqs. (1) and (8) the value of the couplings can be read off, $g_{aa} = g_{bb} = c_0 + c_2$ and $g_{ab} = g_{ba} = c_0 - c_2$.

Once the total number of atoms is fixed, we investigate the Josephson-like dynamics for different numbers of atoms populating each component, $N_a = f_a N$ and $N_b = f_b N$, and for different initial conditions $z_a(0)$, $z_b(0)$, $\delta\phi_a(0)$ and $\delta\phi_b(0)$.

4.1. *Phase coherence and localization*

The numerical solutions of the **GP3D** for the single component system showed two features. First, the atoms remained mostly localized in the two minima of the potential-well and secondly, each group of atoms had to a large extent the same quantum phase. This, clearly supported the picture of having two BEC, one at each side of the barrier, with a well defined phase at each side during the dynamical evolution.

As in the scalar case, our exact **GP3D** numerical solutions of the dynamics of the binary mixture in several initial conditions of population imbalances and phase differences show the same two distinctive features, see Fig. 3. First, the density of atoms for each component is always bi-modal, with the two atom bunches centered around the minima of the potential well. Secondly, the phase of the wave function is mostly constant for each species at each side of the potential trap. Thus, we find that the **GP3D** does predict the dynamics to be mostly bi-modal also for the binary mixture case.

At the end of the section we will consider some deviations from the bi-modal behavior that are found in very specific conditions.

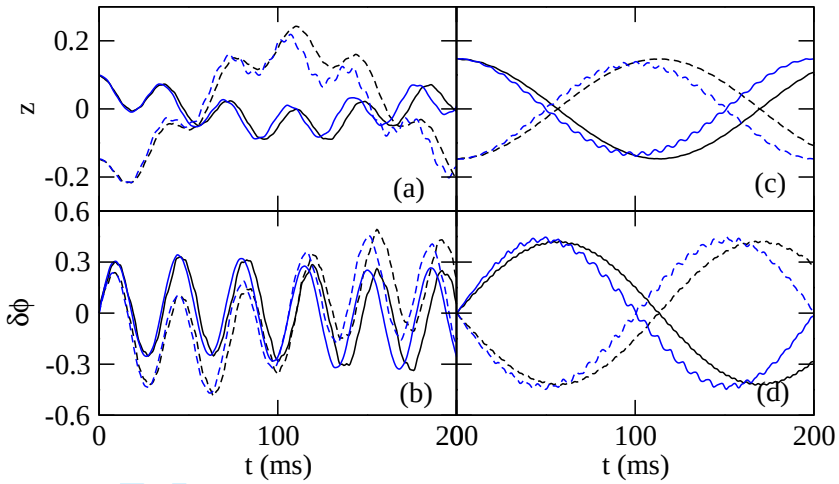

Figure 4. Behavior of the population imbalance, $z_a(t)$ (solid lines), and $z_b(t)$ (dashed lines), and phase difference, $\delta\phi_a(t)$ (solid lines) and $\delta\phi_b(t)$ (dashed lines), computed using **GP3D** (black lines), and **NPSE** (blue lines) in a polarized case, $f_a = 0.8$, left, and a zero polarization case, $f_a = 0.5$, right, respectively. The initial conditions are $z_a(0) = 0.1$, $z_b(0) = -0.15$ and $\delta\phi_a(0) = \delta\phi_b(0) = 0$ for the left panels, and $z_a(0) = -z_b(0) = 0.15$ and $\delta\phi_a(0) = \delta\phi_b(0) = 0$ for the right panels.

4.2. *Rabi and anti-Josephson modes*

The two predictions of the two-mode model described in Refs. [20, 22], namely the "anti-Josephson" behavior, and the enhancement of the Rabi mode, are confirmed by the **NPSE** and **GP1D** simulations as can be seen in Fig. 4. In Fig. 4 (left panels) we consider a very polarized case with $f_a = 0.8$. As expected from two-mode analysis the dynamics of the most populated component should to a large extent decouple from the less populated one and perform fast Josephson oscillations with a frequency close to the corresponding one for the scalar case, $\omega_J = \omega_R\sqrt{1 + NU/(\hbar\omega_R)}$ (where ω_R is the Rabi frequency, that is, the frequency of oscillation of a single atom in the double-well potential). The **GP3D** simulation is seen to confirm the above predictions. The less abundant component is strongly driven by the most populated one and shows an anti-Josephson behavior as described in Ref. [20].

Another prediction is related to the behavior of $z_a + z_b$ and $z_a - z_b$ in the non-polarized case, $f_a = f_b$. As explained in Ref. [22] in this case the difference, $z_a - z_b$, should enhance the long mode which oscillates with the Rabi frequency of the system, while the sum $z_a + z_b$ should mostly oscillate with the Josephson frequency, ω_J. In the right part of Fig. 4 we present the extreme case when $z_a(0) = -z_b(0)$ computed with **GP3D** and **NPSE**. In this case, both population imbalances and phase differences oscillate mostly with the Rabi frequency of the system, keeping during the time evolution $z_a + z_b \sim 0$.

Both 1D reductions produce qualitatively similar physics. The only important difference is that the frequency of the Josephson oscillations is higher in the **GP1D**, as occurred already for the single component [22].

Interestingly, they predict different Josephson oscillations while the Rabi frequencies are similar. The long oscillation corresponding to the Rabi mode is seen to agree well with the corresponding long oscillation seen in the right panels of Fig. 4. The Josephson-like oscillations of binary mixtures of spinor $F = 1$ ^{87}Rb BECs around the $(z_a^0, \delta\phi_a^0, z_b^0, \delta\phi_b^0) = (0, 0, 0, 0)$ are therefore essentially controlled by two frequencies, ω_R and ω_J.

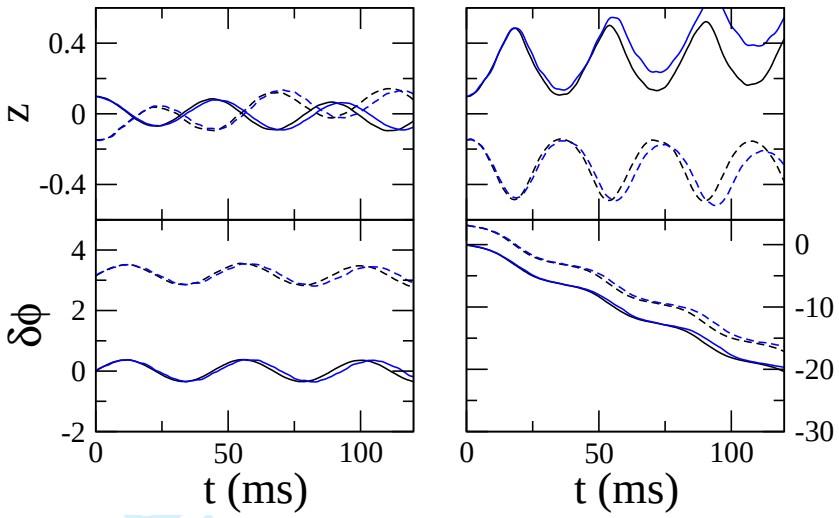

Figure 5. Two simulations with the same initial conditions, $z_a(0) = 0.1$, $z_b(0) = -0.15$, $\delta\phi_a(0) = 0$ and $\delta\phi_b(0) = \pi$ but with different compositions of the mixture. The case on the left has $f_b = 0.2$ while the case on the right $f_b = 0.8$. The blue lines are obtained by means of a full **GP3D** and the black lines are the **NPSE** results. Solid and dashed lines correspond to the a and b components, respectively.

4.3. *Small oscillations around $z^0_{a,b}$, $\delta\phi^0_a = 0$ and $\delta\phi^0_b = \pi$; Effects beyond two-mode.*

As explained in detail in Ref. [22], the dynamics for these conditions depend on the specific value of f_b considered. The trivial equilibrium point at $z_i = 0$ exists provided $f_b \lesssim 0.43$ [22]. This prediction of the two-mode models is observed both in the **GP3D** and **NPSE** as it can be seen in Fig. 5. In the figure, we consider a simulation with $z_a(0) = 0.1$, $z_b(0) = -0.15$, and $f_b = 0.2 < 0.43$ (left panels). The population imbalance (upper panel) of both components oscillates in the usual Josephson regime. At the same time, the phase difference oscillates with its characteristic phase-shift of $\pi/2$ with respect to the imbalance (lower panel). The phase of the a component oscillates around $\delta\phi_a = 0$ while $\delta\phi_b$ does oscillate around $\delta\phi_b = \pi$.

A completely different picture emerges when the fraction of atoms in both components is exchanged, $f_b = 0.8 > 0.57$ (right panels), with most of the atoms populating the b component. In this case, the oscillation amplitude is large, both components remain trapped on their original sides and the phase difference becomes unbounded. This should be considered as a genuine effect of the binary mixture as each component follows a running phase mode at each side of the potential barrier.

Again, the comparison between the **NPSE** and **GP3D** is very satisfactory. The **NPSE** captures almost completely the dynamics up to times of 100 ms. In all cases, the **NPSE** reproduces correctly both the phase difference and population imbalance. The only sizeable discrepancies occur for times $\gtrsim$ 80 ms in the run without equilibrium point (right panel).

An example of simulations around non-trivial equilibrium points is presented in Fig. 6. These points involve very large and opposite initial population imbalances for both components. In Fig. 6 we consider a case with initial conditions very close to the predicted equilibrium point using the standard two-mode, $z_a(0) = -0.78$, and $z_b(0) = 0.99$, with $f_a = 0.1$. Also in the same figure we consider a similar run but with $f_a = 0.9$. In both cases the **NPSE** and **GP3D** predict a very similar dynamics.

Most of the dynamics described up to now can to a large extent be understood within two-mode models [22]. There are, however, a number of situations where the two-mode fails. Some are a direct consequence of having two components evolving

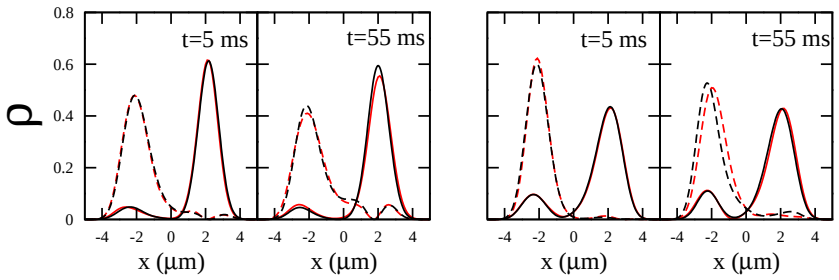

Figure 6. Two simulations with the same initial conditions, $z_a(0) = -0.78$, $z_b(0) = 0.99$, $\delta\phi_a = 0$ and $\delta\phi_b = \pi$, but with different composition. The case on the left has $f_a = 0.1$ while the case on the right $f_a = 0.9$. The red lines are obtained by means of a full **GP3D** while the black lines are the **NPSE** results. Solid and dashed lines correspond to the a and b components, respectively.

in the same double-well potential, others are due to having initial configurations, mostly with large initial imbalances, producing situations where the atom-atom interaction energy per atom is comparable to the gap between the first excited state and the second/third excited states.

We can distinguish two different cases: (a) involving excitations along the coordinate which contains the barrier, (b) involving excitations of the transversal coordinates.

An example of (a) is shown in Fig. 6. There, as clearly seen in the density profiles along the x direction, the two-mode approximation is no longer valid. The simplest way of seeing this is by noting the zero in the density of one of the components at $x \sim 2\mu$m. This effect beyond two-mode is well taken care of by the **NPSE** which reproduces the density profile quite well during most of the time evolution considered in the simulation. Thus, the excitations of higher modes along the direction which has not been integrated out in the 1D reduction do not pose a great difficulty to the 1D reductions.

The second type of effects beyond two-mode, (b), involve excitations of the transverse components. These effects are present in any binary mixture calculation whenever the intra- and inter-species interactions are not equal, see for instance the last section of [22].

5. Conclusions

The rich dynamical regimes which take place in binary mixtures, like double self-trapped modes, Josephson oscillations, or zero- and π-bound phase modes, have been studied by performing full **GP3D** simulations covering all the relevant initial conditions. The 3D numerical solutions of the Gross-Pitaevskii equations have been used to critically discuss the validity of the most common 1D reductions of the GP equations, **GP1D** and **NPSE** .

To fix the conditions of the dynamics, we have focused in one particular setup that corresponds to a natural extension of the experiments reported in Ref. [2]: the case of a binary mixture made by populating two of the Zeeman states of an $F = 1$ ^{87}Rb condensate. As discussed in the present paper, this setup already allows to observe and characterize a large variety of phenomena which are genuine of the binary mixture, e.g. anti-Josephson oscillations in highly polarized cases, long Rabi-like oscillating modes, zero- and π-locked modes, etc.

Two commonly employed dimensional reductions of the **GP3D** , the **GP1D** and **NPSE** , have been shown to differ substantially among each other, with the **NPSE** being clearly in much better agreement with the original 3D dynamics in a broader set of conditions. In general, the **GP1D** describes essentially the correct

physics but quantitatively far from the **GP3D** predictions. Also, for self-trapped cases already in the single component case, it departs from the two-mode behavior earlier than the **GP3D** or the **NPSE** . The agreement between the **NPSE** and the full 3D dynamics is astonishingly good both for single component and the considered binary mixtures, where the intra- and inter-species are very similar and the **NPSE** equations are particularly easy to handle. This agreement is not only seen on fully integrated magnitudes, for instance population imbalances, but also on the density profiles predicted along the direction hosting the barrier.

Acknowledgments

We thank J. Martorell for useful discussions. B.J-D. is supported by Grup Consolidat SGR 21-2009-2013. M. M-M is supported by an FPI PhD grant of the Ministerio de Ciencia e Innovación (Spain). This work is also supported by the Grants No. FIS2008-00421, FIS2008-00784 and FIS2008-01236 from MEC (Spain), and Grants No. 2009SGR-01289 and 2009SGR-0985 from Generalitat de Catalunya.

References

[1] M. R. Andrews, C. G. Townsend, H.-J. Miesner, D. S. Durfee, D. M. Kurn, and W. Ketterle, Science **275**, 637 (1997).
[2] M. Albiez, R. Gati, J. Fölling, S. Hunsmann, M. Cristiani, and M. K. Oberthaler, Phys. Rev. Lett. **95**, 010402 (2005).
[3] S. Levy, E. Lahoud, I. Shomroni, and J. Steinhauer, Nature **449**, 579 (2007).
[4] T. Zibold, E. Nicklas, C. Gross, M. K. Oberthaler, Phys. Rev. Lett. **105**, 204101 (2010).
[5] A. Smerzi, S. Fantoni, S. Giovanazzi, and S. R. Shenoy, Phys. Rev. Lett. **79**, 4950 (1997).
[6] G.J. Milburn, J. Corney, E. M. Wright, and D. F. Walls, Phys. Rev. A **55**, 4318 (1997).
[7] R. Gati and M. K. Oberthaler, J. Phys. B: At. Mol. Opt. Phys. **40**, R61 (2007).
[8] K. Sakmann, A. I. Streltsov, O. E. Alon, and L. S. Cederbaum, Phys. Rev. Lett. **103**, 220601 (2009).
[9] B. Juliá-Díaz, D. Dagnino, M. Lewenstein, J. Martorell, and A. Polls, Phys. Rev. A **81**, 023615 (2010).
[10] D. Ananikian and T. Bergeman, Phys. Rev. A **73**, 013604 (2006).
[11] L. Salasnich, A. Parola, and L. Reatto, Phys. Rev. A **65**, 043614 (2002).
[12] S. Ashab and C. Lobo, Phys. Rev. A **66**, 013609 (2002).
[13] H. T. Ng, C. K. Law, and P.T. Leung, Phys. Rev. A **68**, 013604 (2003); L. Wen and J. Li, Phys. Lett. A **369**, 307 (2007).
[14] X-Q. Xu, L-H. Lu and Y-Q. Li, Phys. Rev. A **78**, 043609 (2008).
[15] B. Sun and M. S. Pindzola, Phys. Rev. A **80**, 033616 (2009).
[16] A. Naddeo, R. Citro, J. Phys. B: At. Mol. Opt. Phys. **43**, 135302 (2010).
[17] G. Mazzarella, M. Moratti, L. Salasnich, and F. Toigo, J. Phys. B: At. Mol. Opt. Phys. **43**, 065303 (2010).
[18] C. Wang, P. G. Kevrekidis, N. Whittaker and B. A. Malomed, Physica D **327**, 2922 (2008).
[19] I. I. Satija, R. Balakrishnan, P. Naudus, J. Heward, M. Edwards, and C. W. Clark, Phys. Rev. A **79**, 033616 (2009).
[20] B. Juliá-Díaz, M. Guilleumas, M. Lewenstein, A. Polls, and A. Sanpera, Phys. Rev. A **80**, 023616 (2009).
[21] W. Wang, J. Phys. Soc. Jpn.78, 9, 094002 (2009).
[22] M. Melé-Messeguer, B. Juliá-Díaz, M. Guilleumas, A. Polls and A. Sanpera, New Journal of Physics **13**, 033012 (2011).
[23] S. K. Adhikari, J. Phys. B: At., Mol. Opt. Phys. **44**, 075301 (2011).
[24] M. Olshanii, Phys. Rev. Lett. **81**, 938941 (1998).
[25] W. Zhang, and L. You, Phys. Rev. A **71**, 025603 (2005).
[26] L. Salasnich and B. A. Malomed, Phys. Rev. A **74**, 053610 (2006).
[27] T.-L. Ho, Phys. Rev. Lett. **81**, 742 (1998); T. Ohmi and K. Machida, J. Phys. Soc. Jpn. **67**, 1822 (1998); M. Moreno-Cardoner, J. Mur-Petit, M. Guilleumas, A. Polls, A. Sanpera, and M. Lewenstein, Phys. Rev. Lett. **99**, 020404 (2007).
[28] E. G. M. van Kempen, S. J. J. M. F. Kokkelmans, D. J. Heinzen, and B. J. Verhaar, Phys. Rev. Lett. **88**, 093201 (2002).